energy&fuels

Article

pubs.acs.org/EF

Biochar from Slow Pyrolysis of Two-Phase Olive Mill Waste: Effect of Pressure and Peak Temperature on its Potential Stability

Joan J. Manyà,* Sergio Laguarta, Miguel A. Ortigosa, and José A. Manso

Thermo-chemical Processes Group (GPT), Aragón Institute of Engineering Research (I3A), University of Zaragoza, Technological College of Huesca, Carretera Cuarte s/n, E-22071 Huesca, Spain

ABSTRACT: The present study examines the effect of both the pressure and peak temperature on the potential stability of the biochar produced from the slow pyrolysis of two-phase olive mill waste. On the basis of the available studies in the literature, the following properties were taken as rough indicators of the potential stability of biochars in soils: the fixed-carbon yield, the fraction of aromatic C, and the molar H:C and O:C ratios. Pyrolysis experiments were performed in a laboratory-scale fixed-bed device and planned following a central composite design. The product gas yield and composition values at the outlet of the secondary cracking reactor (a fixed-bed of activated alumina particles at 700 °C) were also analyzed as a function of pressure and peak temperature. The results from the statistical analyses indicate that both the analyzed factors have a strong influence on the distribution of the pyrolysis products, as well as on the properties of the produced biochar. The most potentially stable biochars were obtained at the highest values of pressure and peak temperature (1.1 MPa and 600 °C). A positive effect of the pressure on the pyrolysis gas yield (at the expense of the total liquid fraction) was also observed.

1. INTRODUCTION

In recent years, biochar has received increasing attention as a promising way to simultaneously sequester carbon and improve soil fertility.[1−3] Biochar is usually produced by conventional carbonization or slow pyrolysis of biomass because of the ability of this thermochemical process to increase the charcoal yield.[4] Despite the fact that a growing number of research studies are currently focused on the effects of biochar on soil properties and functions, relatively little attention has been directed toward the establishment of the appropriate process conditions to obtain a charcoal with suitable properties for biochar purposes.[3,5]

Among the most important factors affecting the slow pyrolysis process, the peak temperature and pressure can play a crucial role in both the biochar yield and fixed-carbon content. Peak temperature is defined as the highest temperature reached during the pyrolysis process.[6] As a general trend, the biochar yield decreases as the peak temperature rises.[7−11] However, an increase in the peak temperature leads to a progressive increase in the fixed-carbon content.[6,12−15] In several recently published studies,[10,13,14,16−19] the effect of the peak temperature on several properties of biochar that are related to its potential application as a soil amendment and carbon sequestration agent was examined. The results from these studies, which were performed for several biomass feedstocks, revealed that an increase in the peak temperature (from 400 to 600 °C in the most of cases) resulted in an increase in the proportion of aromatic C[14,16,17] and/or the aromatic C cluster size.[18] In addition to this, a decrease in both H:C and O:C ratios with rising the peak temperature was also reported.[13,18,19] These findings suggest that increasing the peak temperature may improve the chemical recalcitrance of the biochar, that is, its ability to resist abiotic and biotic degradation.

In regard to the effect of the pressure, previous studies reported that both the charcoal yield and fixed-carbon content were higher when a moderate pressure (0.5−3.0 MPa) was applied during the pyrolysis process.[20−23] Antal and Gronli[6] attributed this behavior to an increase in the vapor residence time, within and in the vicinity of the particle, with pressure. This situation results in an increase in the biochar yield because of the major role of the secondary reactions (by means of which additional charcoal is produced by repolymerization of the tarry vapors). As can be expected, this improvement in the biochar yield become more pronounced at lower gas flow rates (through the particle bed). At this point, an interesting question may arise: which of these two linked factors (pressure or gas residence time) is the most responsible for differences in biochar yield? This uncertainty could explain some apparently contradictory results reported in different studies,[15,24−28] in which a negligible (or even negative) effect of the pressure on the biochar yield was reported. Whitty and co-workers[27] observed very little difference in char yields from a feedstock of black liquor at temperatures below 800 °C and pressures of 1.0 and 2.0 MPa. From the work conducted by Mahinpey and co-workers[28] on the pressurized pyrolysis of wheat straw, no difference in the yield of char was reported. In line with these findings, Melligan and co-workers[24] also observed a nearly constant char yield as a function of pressure (in the range of 0.1−2.6 MPa) during pyrolysis of miscanthus at a peak temperature of 550 °C. In the case of the study of Manyà and co-workers,[15] who reported a statistically significant decrease in the biochar yield with pressure, the authors suggested that the configuration of the experimental device (a pressurized TGA system), wherein the volatiles were quickly removed from the reaction chamber, could explain their findings. In any case, the intrinsic effect of pressure on the biochar yield needs to be

Received: March 24, 2014
Revised: April 4, 2014
Published: April 7, 2014

clarified by performing, for instance, pyrolysis tests at a constant gas-phase residence time.

In reference to the effect of the pressure on the potential stability of the produced biochar, little information is available in the literature. Melligan and co-workers[24] observed a progressive decrease in both the H:C and O:C ratios and a parallel increase in the proportion of aromatic C when the pressure was varied from atmospheric to 2.6 MPa in steps of 0.5 MPa. In other words, increasing the pressure may also result in improving the potential stability of the produced biochar.

In addition to the operating conditions, the physicochemical properties of the biomass feedstock (such as particle size, moisture content, ash content and composition, and extractives and lignin contents) can also affect the behavior of the pyrolysis process.[6,14,29] This fact limits the generalization of the conclusions resulting from the experimental studies focused on a given biomass feedstock.

Two-phase olive mill waste (TPOMW) is an acidic wet solid waste, the disposal of which is a major problem in the olive oil industry.[30,31] In order to clarify the results obtained in the above-mentioned earlier study[15] (especially those related to the effect of pressure on the biochar yield) and investigate the effect of both the pressure and peak temperature on the potential stability biochar, the present study adopted a central composite design of experiments. Experimental runs were conducted in a pressurized fixed-bed reactor system under a nitrogen atmosphere, the mass flow rate of which was continuously adjusted in order to keep the gas residence time inside the pyrolysis reactor constant and thus measure the intrinsic effect of pressure.

Table 1. Proximate, Elemental, and XRF Analyses of the TPOMW Samples

proximate (wt %)	
moisture	16.85 ± 0.95
ash	2.27 ± 0.07
volatile matter	63.61 ± 0.48
fixed carbon	17.27 ± 1.36
ultimate (wt % daf)	
C	42.0 ± 1.05
H	5.99 ± 0.06
N	3.18 ± 0.12
S	<0.1
inorganic matter expressed as percentage of oxides (wt % of ash)	
CaO	42.1
K_2O	26.4
SiO_2	10.0
Fe_2O_3	6.90
Al_2O_3	3.91
P_2O_5	3.90
MgO	1.69
TiO_2	0.476
PbO	0.256
SnO_2	0.231
CuO	0.221
MnO	0.196
ZnO	0.137
SO_3	2.95
Cl	0.251

2. EXPERIMENTAL SECTION

2.1. Biomass Feedstock. The TPOMW samples were supplied by an extra-virgin olive oil factory located in the Spanish region of Aragón. In that factory, two-phase olive mill wastes were sun-dried in the field for several months. The as-received material was broken in a jaw crusher and sieved to obtain a particle size in the range of 0.15−1.0 cm. The characterization results (proximate, elemental, and X-ray fluorescence (XRF) analyses) are given in Table 1.

2.2. Fixed-Bed Pyrolysis System and Procedure. Figure 1 shows the schematic diagram of the experimental system that was designed to operate at internal temperatures (in the pyrolysis reactor) up to 800 °C and absolute pressures up to 1.5 MPa. The pyrolysis reactor consists of a vertical tube (40.9 mm inner diameter; 500 mm long) made of high temperature austenitic stainless steel (Outokumpu 253; EN 1.4835). This reactor was heated by a 1.5 kW electric resistance with proportional integral derivative (PID) temperature control. The evolved permanent gases and vapors from the pyrolysis reactor were transferred to the cracking reactor (a vertical tube of 20.9 mm inner diameter and 250 mm long, made of ASTM 316L stainless steel, and electrically heated with a 0.5 kW resistance), which consists of a fixed-bed of alumina porous particles at an inlet temperature of about 700 °C. The activated aluminum oxide used in this study was Compalox AN/V-812 (particle size ranged from 1.0 to 2.5 mm; Brunauer−Emmett−Teller (BET) specific surface area of 230−300 m^2 g^{-1}) from Albemarle (Germany). The goal of the cracking reactor is to minimize the amount of tar contained in the exit gas stream. To retain any solid particle, a downstream filter consisting of an ASTM 316L stainless steel tube that holds a glass fiber thimble was used. The temperature inside the filter, as well as on the trace-heated connecting tubes, was kept at 450 °C to avoid tar condensation. The liquid product was condensed in a glass trap immersed in an ice−water bath. The glass trap was carefully weighted before and after each experimental run to estimate the total liquid (water + tar) yield.

A back pressure regulator was used to maintain the pressure of the system at a desired value. The nitrogen mass flow rate (measured at normal conditions (NTP)) through the pyrolysis reactor was adjusted as a function of the absolute pressure and bed temperature (measured by means of a K-type thermocouple placed at the cylinder axis and 5 cm from the bottom of the reactor) to maintain the superficial gas velocity constant at a value of 0.015 m s^{-1}, which results in an average space velocity (GHSV) of 216 h^{-1} (assuming a void fraction of 0.5). Under this flow condition, the GHSV values in the secondary reactor were in the range of 1230−1595 h^{-1}.

For each experimental run, 75 g of TPOMW (which occupies around 40% of the reactor volume with a bed height of around 200 mm) was charged to the fixed-bed pyrolysis reactor at room conditions. After checking for absence of leaks, the system was pressurized with nitrogen at the desired pressure. The N_2 flow rate was continuously adjusted by means of a needle valve and monitored by a mass flow meter. The inert gas was heated to 350 °C in a preheater unit (a coiled tube with a resistive wire of 0.2 kW) and then fed to the pyrolysis reactor through the distribution plate. The pyrolysis reactor was heated to the desired peak temperature at a heating rate of about 5 K min^{-1}. Permanent gases were collected from the outlet of the cleaning system by means of 1 L Tedlar gas bags. The first gas sample was taken when the inlet temperature of the pyrolysis reactor reached 250 °C. The successive samples were collected every 50 °C increase in the pyrolysis reactor temperature. The gaseous products were analyzed using a micro gas chromatograph (μ-GC Varian CP-4900) equipped with two independent channels and thermal conductivity detectors.

Each experimental run was completed 1 h after the pyrolysis peak temperature was reached. During the natural cooling of the device, the N_2 flow was maintained to prevent charcoal oxidation. Once the pyrolysis reactor reached room temperature, the gas flow was turned-off and the system depressurized. The liquid fraction and biochar were then weighted to determine the respective yields. The water content in the liquid product was measured by Karl Fischer titration, whereas the gas yield was estimated from the overall mass balance.

2.3. Biochar Characterization. All of the obtained biochars were characterized by proximate and elemental analyses following the same procedures as described for the TPOMW samples. The pH of the

dx.doi.org/10.1021/ef500654t | Energy Fuels 2014, 28, 3271−3280

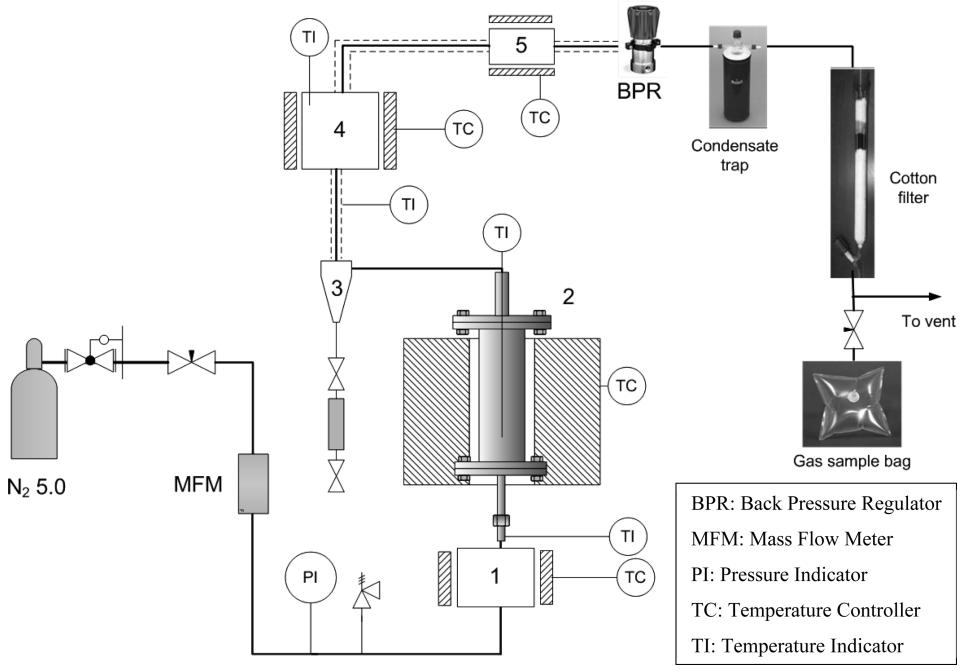

Figure 1. Schematic diagram of the experimental system: (1) preheater, (2) fixed-bed pyrolysis reactor, (3) cyclone, (4) cracking reactor, and (5) hot filter.

biochars was measured in deionized water at 1:5 (w/w) ratio after stirring for 1 h.[32] Solid-state ^{13}C cross polarization and magic angle spinning (CP-MAS) nuclear magnetic resonance (NMR) spectra were obtained for all the biochar samples using a Bruker Avance 400 (Bruker Corp., Germany) spectrometer at a frequency of 100 MHz. From the experimental NMR spectrum and according to McBeath and co-workers,[16] the proportion of aromatic C was estimated as the ratio of the area under the aromatic peaks to the total area of the spectrum. A preliminary deconvolution procedure, consisting in fitting the experimental signal as the sum of multiple Gaussian peaks, was carried out using the "Peak Analyzer" tool implemented in OriginPro version 8.5 (OriginLab, Northampton, MA). The fitted peaks were assigned as aromatic ones in the case that the center of the peak was in the chemical shift range of 110−165 ppm.

The proportion of aromatic C deduced from the NMR spectra seems to be a good predictor of the potential stability of biochar in the soil.[3] In this sense, Singh and co-workers[33] recently reported that both the proportion of biochar C mineralized and the estimated mean residence time of biochar in the soil are positively and nonlinearly correlated with the proportion of aromatic C and the degree of aromatic C condensation.

2.4. Design of Experiments. A two-level face-centered central composite design (FCCCD) was adopted in the present study to statistically analyze the effects of the selected factors (absolute pressure and peak temperature).[34] This type of design is appropriate to build a second-order response surface model. The RcmdrPlugin.DoE package[35] within the R environment (version 3.0.1) was used to create the design of experiments and conduct the relevant statistical analyses. The matrix of the applied design is shown in Table 2. As previously mentioned in section 2.2, the rest of operating conditions in the pyrolysis reactor were kept constant during all of the pyrolysis runs (N_2 superficial gas velocity, heating rate, particle size, amount of TPOMW initially loaded, and solid residence time at the peak temperature). Taking into account that two batches of raw TPOMW (obtained from the same facility but at different dates) were required to complete the experimental work, the design of experiments was blocked into two blocks in order to statistically analyze the effect of the batch used (nuisance factor).

Six response variables related to biochar characteristics were statistically analyzed: the mass yield in a dry basis (y_{char}), the fixed-carbon yield (y_{FC}) in a dry and ash-free basis, the molar H:C ratio, the molar O:C ratio, the percentage of aromatic C, and the pH. The molar H:C and O:C ratios were calculated from the elemental composition. According to Antal and co-workers,[12] the fixed-carbon yield was calculated using eq 1.

$$y_{FC} = \left(\frac{m_{char}}{m_{bio}}\right)\left(\frac{\%FC}{100 - \%ash}\right) \quad (1)$$

where %FC and %ash are the percentage of fixed-carbon present in the biochar and the percentage of ash in the feedstock, respectively. The ratio between m_{char} (mass of produced biochar) and m_{bio} (dry mass of feedstock) corresponds to the biochar yield (y_{char}). The y_{FC} value is an indicator of the efficiency of the pyrolytic conversion of the ash-free organic matter (initially present in the biomass feedstock) to a

Table 2. Matrix of the 2^2 Face-Centered Central Composite Design Adopted in the Present Study

	factors	
	x_1	x_2
level	pressure (MPa)	peak temperature (°C)
low (−1)	0.1	400
middle (0)	0.6	500
high (+1)	1.1	600

	factors		
run	x_1	x_2	block
1	−1	−1	1
2	0	0	1
3	0	0	1
4	+1	−1	1
5	0	0	1
6	−1	+1	1
7	+1	+1	1
8	0	+1	2
9	+1	0	2
10	0	−1	2
11	−1	0	2
12	0	0	2

dx.doi.org/10.1021/ef500654t | Energy Fuels 2014, 28, 3271−3280

relatively pure, ash-free carbon. Moreover, the content of fixed-carbon could be a measure of the potential stability of biochar. In this sense, Zimmerman[36] found a significant positive correlation between the labile C fractions and the volatile matter content of biochar.

3. RESULTS AND DISCUSSION

The main experimental results are shown in Table 3. Each response variable was analyzed by response surface methodology (RSM)[34] in order to build a regression model that can be able to reflect the quantitative influence of factors. Thus, from the experimental data generated using the above-mentioned FCCCD approach, functional relationships between the response (y) and the coded independent variables (x_1 for pressure and x_2 for peak temperature) can be quantified by means of the estimated parameters of a second-order regression model (eq 2).

$$y = \beta_0 + \sum_{j=1}^{k} \beta_j x_j + \sum_{i<j} \sum \beta_{ij} x_i x_j + \sum_{j=1}^{k} \beta_{jj} x_j^2 + \varepsilon \quad (2)$$

where β_0, β_j, β_{ij}, and β_{jj} are the intercept, linear, interaction, and quadratic coefficients; respectively. Depending on the results of corresponding statistical tests applied to each model, three different scenarios are possible: (a) the linear model is accurate enough, (b) the second-order model is the most appropriate, and (c) a higher order of the model is required. In the following sections, the results of the statistical analysis for each response variable (which are given in Table 4) are presented and discussed. From the data reported in Table 4, it is concluded that the block effects were not significant for any response variable. This outcome suggests that the effect of the TPOMW batch was negligible.

Table 3. Experimental Results Obtained from the Central Composite Design

run	y_{char}	y_{FC}	aromatic C (%)	H:C molar ratio	O:C molar ratio	pH
1	0.8077	0.2332	22.46	1.44	0.54	7.14
2	0.5883	0.2729	36.35	0.95	0.34	7.92
3	0.6360	0.2771	33.58	0.92	0.33	7.83
4	0.6027	0.2506	30.43	0.81	0.38	7.55
5	0.6710	0.2901	34.08	0.94	0.32	7.84
6	0.6276	0.2461	43.68	0.84	0.30	7.19
7	0.4632	0.3180	55.08	0.55	0.18	8.78
8	0.5240	0.2860	47.65	0.73	0.24	8.14
9	0.5715	0.2884	37.26	0.87	0.30	8.09
10	0.6948	0.2435	29.94	0.99	0.36	7.64
11	0.6019	0.2435	37.74	0.96	0.39	7.47
12	0.5505	0.2992	34.90	0.85	0.32	8.01

3.1. Biochar Yield. For this response, the results from the analysis of variance (ANOVA) applied to the linear (with interaction) model indicated that the lack-of-fit was not significant (p-value = 0.512). In addition, the inclusion of the quadratic terms led to a decrease in the adjusted coefficient of determination (R^2_{adj}) from 0.7461 to 0.6586 and an increase of 133% in the predicted residual sums of squares (PRESS). For all of these reasons, the linear model described in Table 4 is the most appropriate fit.

From examining the regression coefficients reported in Table 4 and the contour plot in Figure 2a, it can be concluded that increasing both factors results in a decrease in the biochar yield. The effect of the peak temperature is qualitatively in agreement with a large number of earlier studies.[7,11,14,37−39] However, the negative influence of the absolute pressure (keeping the gas residence time constant) on the biochar yield was not previously reported in the literature. This finding, which is in line with the previous results reported by Manyà and co-workers[15] for pyrolysis experiments conducted for the same biomass feedstock in a pressurized TGA system, suggests that the higher charcoal yields reported in earlier studies[12,21,23] cannot be attributed with complete assurance to the effect of pressure. In other words, the observed higher charcoal yields could also be explained by an increase in the vapor-phase residence time (and a linked decrease in both convective heat and mass transfer rates) in the packed-bed and by additional factors, such as the nature of the biomass feedstock.

As stated by Lédé,[40] the concentration and nature of inorganic species have strong impacts on products properties and yields, possibly as a consequence of their influence on the formation of intermediate species (e.g., intermediate active cellulose) and subsequent reactions. Predicting the behavior of the numerous intermediate species involved is very difficult and still unsolved.[40] It seems reasonable to assume that the evaporation of intermediates to produce volatiles could be inhibited by pressure, leading to the promotion of secondary polymerization reactions. However, during the pressurized experiments reported here, the increase of the N_2 mass flow rate could guarantee a sufficient heat transfer rate[27] to the particles and a sufficient external diffusion rate of the volatiles

Table 4. Summary Statistics for the Most Appropriate Regression Models (Values in Brackets Correspond to the p-values Obtained from the Hypothesis Tests)

response	β_0	β_1	β_2	β_{12}	β_{11}	β_{22}	block	lack-of-fit (F)	R^2_{adj}	PRESS
y_{char}	0.608	−0.066	−0.082	0.010	–	–	0.020	1.20	0.7461	583
	(0.000)	(0.008)	(0.003)	(0.662)			(0.172)	(0.512)		
y_{FC}	0.282	0.022	0.020	0.014	−0.011	−0.012	0.001	1.84	0.8321	22.2
	(0.000)	(0.004)	(0.006)	(0.056)	(0.165)	(0.131)	(0.820)	(0.371)		
molar H:C ratio	0.901	−0.168	−0.187	0.085	–	–	0.021	52.0	0.7975	0.36
	(0.000)	(0.003)	(0.002)	(0.112)			(0.474)	(0.019)		
molar O:C ratio	0.323	−0.062	−0.093	0.010	0.032	−0.013	0.008	14.0	0.8841	0.06
	(0.000)	(0.004)	(0.001)	(0.530)	(0.144)	(0.501)	(0.402)	(0.067)		
aromatic C (%)	35.3	3.15	10.6	0.858	1.14	2.44	−0.795	6.95	0.8656	679
	(0.000)	(0.058)	(0.000)	(0.610)	(0.582)	(0.266)	(0.438)	(0.128)		
pH	7.91	0.437	0.297	0.295	−0.162	−0.052	−0.042	8.05	0.9371	0.86
	(0.000)	(0.000)	(0.001)	(0.003)	(0.067)	(0.070)	(0.272)	(0.112)		

dx.doi.org/10.1021/ef500654t | Energy Fuels 2014, 28, 3271−3280

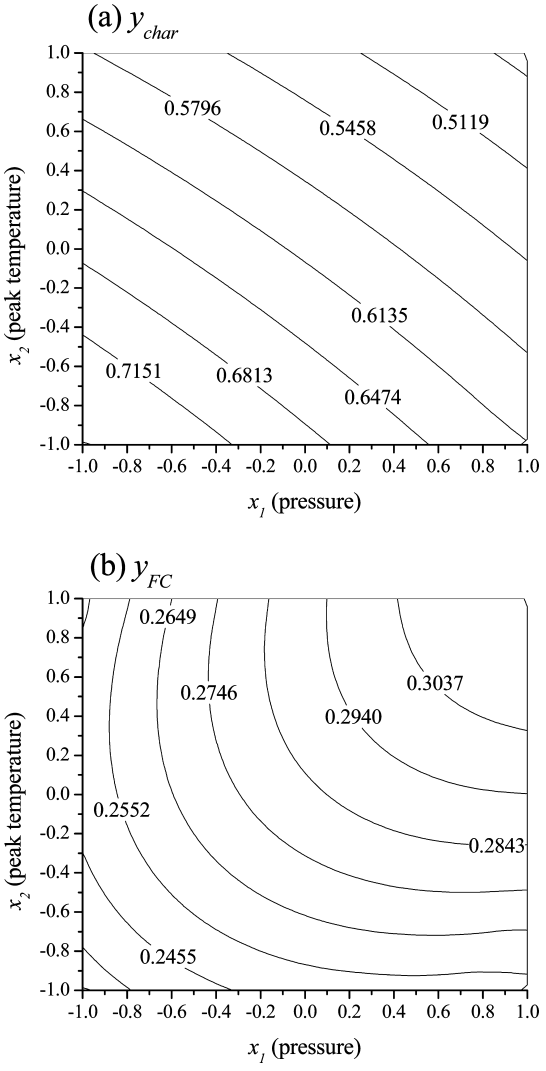

Figure 2. Contour plots showing the effects of the pressure and peak temperature on (a) the biochar yield, and (b) the fixed-carbon yield.

through the bed to maintain the progress of the devolatilization pathway at the expense of volatile recondensation.

An additional explanation for the effect of pressure on the biochar yield could be the fact that steam-char gasification plays a non-negligible role during pressurized pyrolysis experiments. With this respect, several recent studies[41−44] have reported a catalytic effect of the inherent alkali and alkaline earth metallic (AAEM) species on the steam gasification of biochar. In fact, Manyà and co-workers[45] recently reported a significant increase in charcoal yield (in a simultaneous thermogravimetric analysis-differential scanning calorimetry (TGA-DSC) device working at atmospheric pressure) when the same TPOMW samples were washed with hot water to partially remove the inorganic matter. Taking into account that the moisture content of TPOMW samples as well as the contents of K and Ca in the ash are relatively high (see Table 1), it seems reasonable to think that the conversion of carbon through steam gasification could explain the lower biochar yields obtained under pressure. At this point, it should be mentioned that Matsuoka and co-workers[46] observed, for a pressurized fluidized bed of low-rank coal, a significant increase in the steam gasification reaction rate when the partial pressure of the gasifying agent increased in a range of 0.1−0.5 MPa.

In summary, the results reported here might be explained by a combination of multiple causes (specific operating conditions and biomass feedstock nature) that should be fully explored in future studies.

3.2. Fixed-Carbon Yield. For this case, the second-order model was the most appropriate fit (the lack-of-fit was not significant for this model). As can be deduced from the contour plot in Figure 2b, the fixed-carbon yield is maximized when the two factors are at the highest level. In fact, and as can be seen in Table 4, all of the coefficients of the regression model are statistically significant at a confidence level of 90%, except for the quadratic terms (β_{11} and β_{22}). These results concerning the fixed-carbon yield are thus consistent with those available in the literature regarding the favorable effects of the peak temperature[13,14,17] and pressure.[12,15]

Thus, increasing the absolute pressure leads to apparently contradictory results: lower biochar yield but higher fixed-carbon contents. Pressure can enhance the formation of coke from the tarry vapors (yielding to higher fixed-carbon contents in the produced biochar) and simultaneously favor both the overall primary devolatilization and steam gasification processes under the specific operating conditions applied in this study. Further research must continue to prove this hypothesis.

It is interesting to emphasize that the selection of the operating conditions required to maximize the fixed-carbon yield (the highest peak temperature and pressure) also implies the minimization of the biochar yield. This fact confirms the ineffectiveness of the biochar yield as a good indicator of the potential stability of biochar. From the experimental results given in Table 3 and the elemental composition shown in Table 1, it should be noted that, for run #7 ($x_1 = 1$, $x_2 = 1$), 70.8% of the carbon initially present in the biomass feedstock remains as fixed-carbon in the produced biochar. However, for run #1 ($x_1 = -1$, $x_2 = -1$), this percentage drops to 51.9%.

3.3. Molar H:C and O:C Ratios. For the molar H:C ratio, the lack-of-fit was significant at 95% confidence level for both linear and quadratic regression models (p-values of 0.019 and 0.012, respectively). This fact means that a higher order (e.g., cubic) regression model should be more appropriate. Table 4 reports the regression coefficients corresponding to the linear model, which provides a slightly better fit than the second-order model (higher R_{adj}^2 and lower PRESS). In the case of the molar O:C ratio, the second-order model was the most appropriate fit at 95% confidence level. For both response variables, pressure and peak temperature have significant detrimental effects. The observed decrease in the both molar ratios as the peak temperature increases is in agreement with previous studies.[17,19,47] Figure 3a,b shows the contour plots for the molar H:C and O:C ratios, respectively.

It should be noted that the H:C and O:C ratios obtained for the best treatment ($x_1 = 1$, $x_2 = 1$; run #7) are relatively high in comparison to the values reported in earlier studies for biochars produced through slow pyrolysis under atmospheric pressure. For example, Ghani and co-workers[19] measured molar H:C and O:C ratios of 0.33 and 0.06, respectively; for biochars obtained at 550 °C from rubber-wood sawdust. Very similar values were reported by Wu and co-workers[17] (from rice straw at 600 °C), Kim and co-workers[47] (from pitch pine chips at 500 °C), and Keiluweit and co-workers[48] (from pine shavings at 600 °C). However, Enders and co-workers[13] measured molar H:C and O:C ratios of 0.45 and 0.10, respectively; for biochars produced from corn stover at 600 °C. Similar results have recently been reported by Crombie and co-workers[49] for biochars obtained

dx.doi.org/10.1021/ef500654t | Energy Fuels 2014, 28, 3271−3280

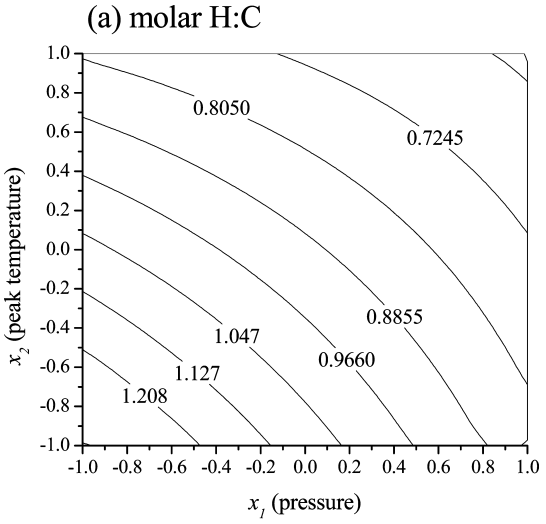

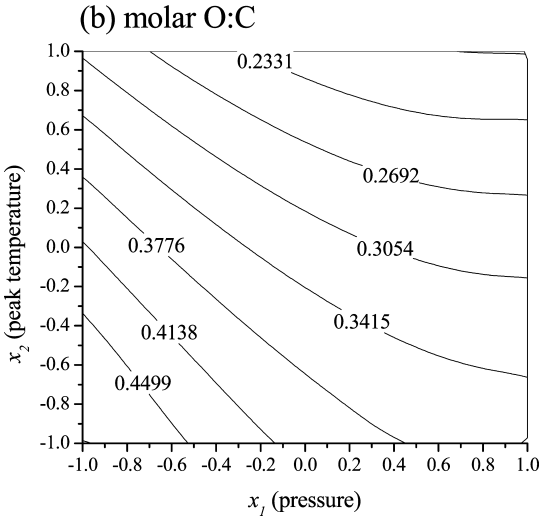

Figure 3. Contour plots showing the effects of the pressure and peak temperature on (a) the molar H:C ratio and (b) the molar O:C ratio.

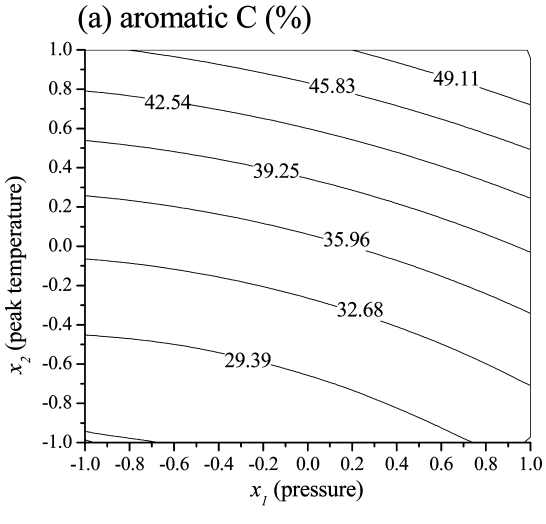

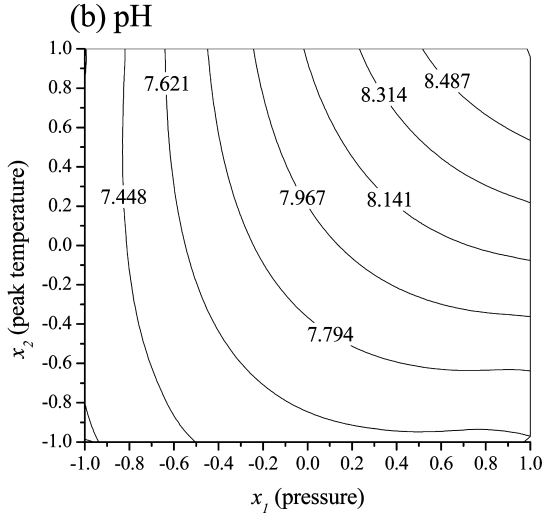

Figure 4. Contour plots showing the effects of the pressure and peak temperature on (a) the percentage of aromatic C and (b) the pH.

from rice husks and wheat straw at a peak temperature of 550 °C. This variability in results could be due to the intrinsic properties of the biomass feedstock (i.e., chemical composition), and probably also due to differences in process conditions during the slow pyrolysis. In this respect, parameters such as the holding time at the peak temperature, the heating rate, and the particle size can play a critical role in the carbonization efficiency, especially in the cases where there are non-negligible heat transfer limitations. This suggestion is supported by the findings reported by Wu and co-workers,[17] who observed a decrease in both the molar H:C and O:C ratios as the holding time increased from 1 to 5 h. A similar trend was also observed by Ronsse and co-workers[50] for various biomass feedstocks pyrolyzed at 600 °C and at two different holding times (10 and 60 min).

3.4. Aromatic C. From the regression coefficients given in Table 4 for the most appropriate fit (second-order model), it can be concluded that an increase in the peak temperature significantly raises the percentage of aromatic C. Pressure also have a positive effect on this response, but at a lower level of confidence (i.e., 94% instead of 99%). In other words, and as can be observed from the contour plot in Figure 4a, the percentage of aromatic C is maximized when the two factors are at the highest level. Figure 5 compares the NMR spectra of the biochars obtained in runs #1 ($x_1 = -1$, $x_2 = -1$), #5 ($x_1 = 0$, $x_2 = 0$), and #7 ($x_1 = 1$, $x_2 = 1$).

As observed for the molar H:C and O:C ratios, the proportion of aromatic C obtained for the best operating conditions (55.08% in run #7) is clearly lower than the values reported in the literature for other biomass feedstocks.[16,17,31,51−53] For instance, McBeath and co-workers[16] reported a 96% of aromatic C for biochars produced from chestnut wood at a peak temperature of 600 °C with a solid residence time at this temperature of 5 h. However, a recent study[14] revealed a wide range of variability in the percentage of aromatic C for biochars produced from several biomass feedstocks at a peak temperature of 500 °C with a holding time of 4 h. This range varied from 47.8% for pig manure-derived biochar to over 80% for wheat straw-derived one. This finding could confirm that the C stability of biochar strongly depends on the nature of the feedstock. In addition, and in light of the results reported here concerning the elemental composition and the proportion of aromatic C, it should be noted that the solid residence time at the peak temperature

dx.doi.org/10.1021/ef500654t | Energy Fuels 2014, 28, 3271−3280

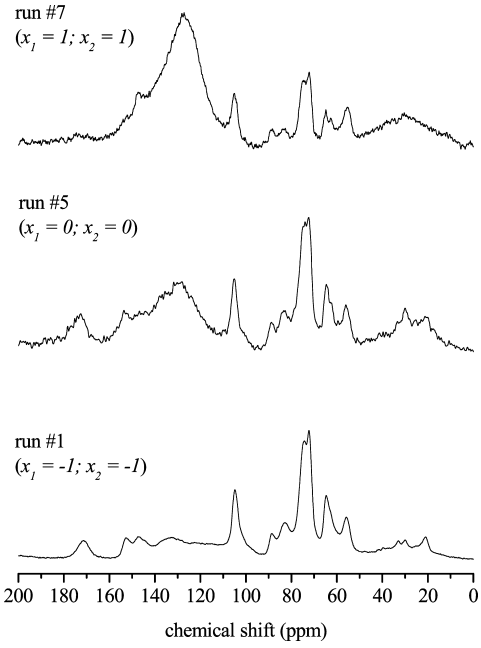

Figure 5. Solid state ^{13}C CP NMR spectra of the biochars obtained in runs #1, #5, and #7.

used in the present study (1 h) was probably too short. In other words, heat transfer limitations at all scales (inter- and intraparticle) were not negligible in practice.

3.5. pH. As can be deduced from Table 4 and Figure 4b, the pH was also maximized for the same values of analyzed factors at which the aromatic C, the molar H:C and O:C ratios, and the fixed-carbon yield were optimized. This fact suggests that these multiple response variables might be correlated with each other. To check this, Table 5 shows the Pearson's correlation matrix among the response variables. As expected, a strong linear correlation was found between the molar H:C ratio and the molar O:C ratio and between the charcoal yield and the fixed-carbon yield. However, the most interesting outcome was the significant correlation between the aromatic C and the rest of variables, including the pH.

Table 5. Pearson's Correlation Matrix for the Response Variables[a]

	y_{char}	y_{FC}	aromatic C (%)	H:C molar ratio	O:C molar ratio
y_{FC}	−0.735				
	(0.006)				
aromatic C (%)	−0.841	0.617			
	(0.001)	(0.032)			
H:C molar ratio	0.921	−0.672	−0.840		
	(0.000)	(0.017)	(0.001)		
O:C molar ratio	0.867	−0.779	−0.894	0.935	
	(0.000)	(0.003)	(0.000)	(0.000)	
pH	−0.794	0.919	0.674	−0.724	−0.799
	(0.002)	(0.000)	(0.016)	(0.008)	(0.002)

[a]Values in brackets correspond to the *p*-values obtained from the hypothesis tests.

According to Lee and co-workers,[54] the alkalinity of biochars depends on three factors: (i) organic functional groups, (ii) carbonates, and (iii) inorganic alkalis. In agreement with previous studies,[10,13,14,17,32,55] the pH values significantly increased with the peak temperature. Zhao and co-workers[14] observed that the pH was predominately controlled by peak temperature and to lesser extent by the biomass feedstock. Enders and co-workers,[13] who measured the pH of 94 biochars obtained from several biomass feedstocks at different peak temperatures, attributed the increase in the pH (to values in the range 7−9) mainly to a decrease in acid functional groups for the low-ash biochars (such as the TPOMW-derived biochars with ash contents below 8%). To support this argument, no correlation has been found between the pH and the ash content for the biochars used here (ρ = −0.187; *p*-value = 0.647). Nevertheless, a decrease in acid functional groups (e.g., carboxylic and phenolic functional groups) can lead to a decrease in the cation exchange capacity (CEC), as reported in earlier studies.[17,56] In other words, the application of the most stable biochar (which also has the maximum pH value) to soil could not be the best choice in terms of optimizing the retention of nutrients (such as NH^{4+}, K^+, and Ca^{2+}). However, further studies are required to investigate the evolution of both the pH and CEC when biochar is added to a given type of soil. Among other variables, the initial acidity of the soil will probably be a key factor in determining the most appropriate biochar from an agronomic point of view.

3.6. Gas Yield and Composition. As an additional aim of the present study, the behavior of several variables related to the liquid and gaseous fractions was analyzed as a function of both the pressure and peak temperature. For this purpose, the responses obtained for the 2^2 factorial design (i.e., corner and center points) were statistically analyzed. Table 6 reports the coefficients of the regression models for the following responses: the mass yields of producer gas and water in a dry basis (y_{gas} and y_{water}, respectively), the concentration of tar in the producer gas (C_{tar}), and the average contents (in vol %) of the major components in the producer gas (in a dry and N_2-free basis).

As can be seen from the regression coefficients reported in Table 6 and the effects graph shown in Figure 6a, the gas yield significantly increases with both the peak temperature and pressure. The increase in the gas yield with the pyrolysis temperature was fully expected because of the thermodynamically and kinetically favored devolatilization process.[7] In regard to the positive effect of the pressure on the gas yield, it could be explained by two facts. First, increasing the pressure can result in a decrease in the liquid fraction at the benefit of permanent gases, as recently reported by Ragucci and co-workers[57] in a study of cellulose pyrolysis in presence of steam. These authors suggest that pressure can enhance the primary degradation of cellulose at low temperatures and also the secondary degradation of condensable species (into permanent gases and secondary charcoal) at higher temperatures. These arguments can also explain the opposite effects of pressure on the biochar and fixed-carbon yields. In addition, the effect of the pressure on the behavior of the secondary cracking reactor should also be considered. In this context, Seshadri and Shamsi[58] reported that an increase in the pressure from 0.1 to 1.7 MPa improved the tar conversion to gaseous products in a fixed-bed of calcined dolomite. Pressure probably improves the adsorption performance of condensable molecules on the activated alumina, increasing their residence time inside the heated reactor. However, and as can be seen from Table 6, the tar content in the exit gas did not significantly decrease with

dx.doi.org/10.1021/ef500654t | Energy Fuels 2014, 28, 3271−3280

Table 6. Summary Statistics for the Linear Regression Models Used to Analyze the Liquid and Gas Yields[a]

response	β_0	β_1	β_2	β_{12}	curvature	R_{adj}^2
y_{gas} (kg kg^{-1} dry biomass)	0.369	0.0959	0.0816	−0.0121	−0.0277	0.9537
	(0.001)	(0.014)	(0.019)	(0.397)	(0.250)	
C_{tar} (mg m^{-3} NTP $_{db}$)	504	−21.0	−29.0	56.5	158	0.8191
	(0.002)	(0.441)	(0.318)	(0.124)	(0.043)	
y_{water} (g kg^{-1} dry biomass)	3.324	−0.874	0.590	−0.359	−0.575	0.9130
	(0.002)	(0.026)	(0.054)	(0.130)	(0.120)	
CO_2 (% vol)	26.95	1.631	0.499	−0.310	1.376	0.5302
	(0.000)	(0.111)	(0.490)	(0.654)	(0.269)	
CO (% vol)	30.67	−6.622	−2.086	1.359	−6.184	0.9962
	(0.000)	(0.001)	(0.010)	(0.022)	(0.003)	
H_2 (% vol)	22.26	0.364	2.839	−2.202	−0.025	0.9879
	(0.000)	(0.154)	(0.003)	(0.005)	(0.930)	
CH_4 (% vol)	20.12	4.627	−1.252	1.153	4.833	0.9812
	(0.000)	(0.005)	(0.063)	(0.073)	(0.011)	

[a]Values in brackets correspond to the *p*-values obtained from the hypothesis tests.

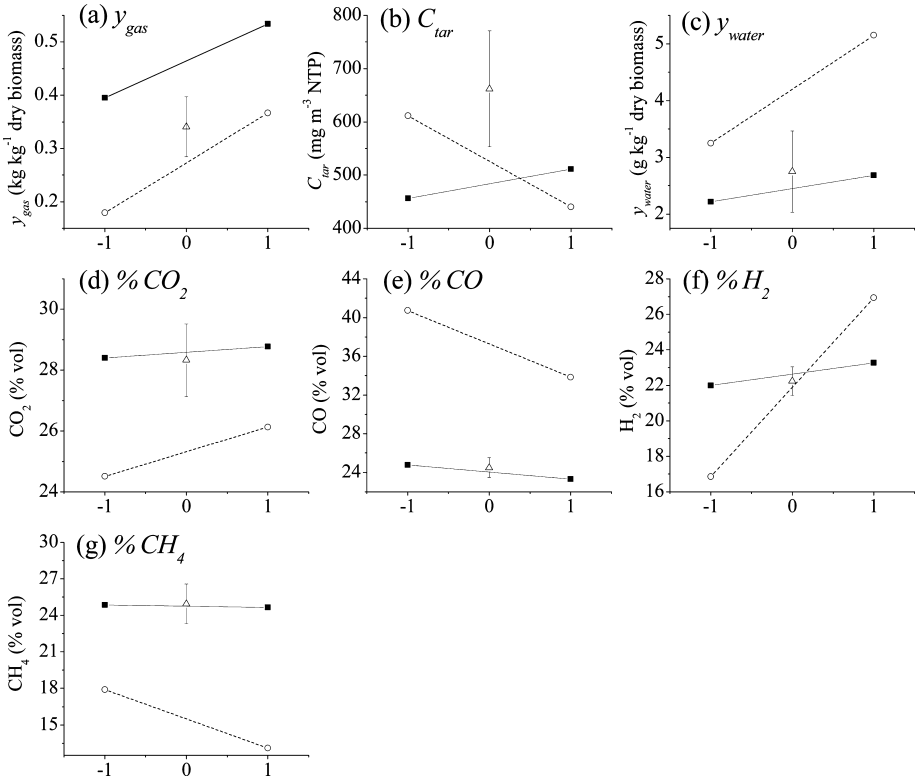

Figure 6. Interaction Effects Plots for (a) y_{gas}, (b) C_{tar}, (c) y_{water}, (d) % CO_2, (e) % CO, (f) % H_2, and (h) % CH_4 against x_2 (peak temperature). The solid and dashed lines correspond, respectively, to the high (x_1 = 1) and low (x_1 = −1) levels of pressure.

pressure. Moreover, the curvature term was significant, indicating that the highest tar concentration could be obtained at intermediate levels of the both analyzed factors. This apparently contradictory result could be due to an effect of the pressure on the coke deposition and consequent changes in the pore size and structure. In any case, these preliminary results point out the potential of the porous alumina as a low-cost alternative for tar removal by thermal cracking. The results reported here for the total tar composition at the outlet of the cracking reactor (less than 800 mg m^{-3} NTP) are promising, although further research is needed to analyze the tar components and determine how to decrease the tar content below 100 mg m^{-3} NTP (the recommended maximum value for applying pyrolysis gas to internal combustion engines).[59] Among the different ways proposed to improve the tar conversion, increasing the bed temperature, adding an oxidation agent and decreasing the space velocity should be investigated.

A significant decrease in the water yield with pressure was also observed in the present work. This finding can be related to the above-discussed increase in the gas yield in the pyrolysis reactor at higher pressure and, additionally, to the behavior of the multiple reactions involved in the cracking reactor. In this sense, an increase in pressure leads to a significant increase in the yield of methane, as can be seen in Figure 6g, probably due to the promotion of the methanation reaction (the reverse reaction of steam methane reforming). Thus, the water generated by methanation can increase the steam-to-CO ratio

dx.doi.org/10.1021/ef500654t | *Energy Fuels* 2014, 28, 3271−3280

and promote the water−gas shift reaction. This interpretation can also explain the results obtained for the CO contents (see Figure 6e), which clearly decreased at high pressure. At a lesser extent than CO, an increase in pressure also leads to a decrease in the hydrogen content in the outlet gas at higher peak temperature (as shown in Figure 6f), probably due to a higher H_2 consumption during the methanation reaction.

4. CONCLUSIONS

With the help of a central composite design of experiments approach, the effects of the pressure and peak temperature on several response variables related to the potential stability of biochar have been objectively evaluated. On the basis of the results obtained from the associated statistical tests, the following conclusions can be drawn: (1) the biochar yield significantly decreases when the pressure increases, keeping the gas residence time inside the pyrolysis reactor constant. Both the pressure and peak temperature have favorable effects on the fixed-carbon yield, that is, on the fraction of the carbon initially contained in the biomass feedstock that remains in the biochar as a potentially stable form. Hence, increasing both operating parameters can result in an increase in the long term C sequestration potential of biochar. (2) The fraction of aromatic C in the biochar strongly increases with peak temperature and, at a lesser extent, with pressure. Working at the highest levels of pressure and peak temperature (1.1 MPa and 600 °C) leads to the production of the most potentially stable biochars. (3) The effects of the evaluated factors on all of the responses related to the potential stability of the obtained biochars (i.e., fixed-carbon yield, aromatic C, and H:C and O:C ratios) are statistically consistent (i.e., no contradictory findings are observed). This fact could confirm the usefulness of the used responses as indicators of the potential stability of biochar. (4) The relatively lower values obtained for the fraction of aromatic C (and also for both molar H:C and O:C ratios) suggest that the solid residence time at the peak temperature was relatively short. Thus, the effect of this variable needs to be carefully investigated in further studies. (5) The biochar pH is linearly correlated with the aromatic C fraction and the molar H:C and O:C ratios; thus, the most potentially stable TPOMW-derived biochars have the highest pH values. This increase in the pH could be mainly due to a decrease in the acid functional groups, which can result in a decline in the cation exchange capacity. (6) Pressure has also a positive effect on the pyrolysis gas production at the expense of the liquid fraction. The fraction of methane in the producer gas significantly increases with pressure due to the promotion of the methanation reactions. Regarding the appropriateness of using a fixed-bed of activated alumina for tar removal, further research is required to determine the best operating conditions yielding to the highest tar conversion.

AUTHOR INFORMATION

Corresponding Author

*J. J. Manyà. E-mail: joanjoma@unizar.es

Notes

The authors declare no competing financial interest.

ACKNOWLEDGMENTS

J.J.M. gratefully acknowledges financial support from the University of Zaragoza (Project UZ2012-TEC-04). The authors gratefully thank Dr. Ignacio Delso for his excellent work in performing the NMR measurements.

NOMENCLATURE

C_{tar} = concentration of tar in the producer gas (mg m^{-3} NTP moisture and N_2 free basis)
F = ratio of the mean regression sum of squares divided by the mean error sum of squares
GHSV = gas hourly space velocity (h^{-1})
m_{bio} = dry mass of TPOMW sample (kg)
m_{char} = mass of produced biochar (kg)
PRESS = predicted residual sums of squares
R_{adj}^2 = adjusted coefficient of determination
x_1 = coded variable for pressure
x_2 = coded variable for peak temperature
y_{char} = biochar yield (kg kg^{-1} of biomass in a dry basis)
y_{FC} = fixed-carbon yield (kg kg^{-1} of biomass in a dry and ash-free basis)
y_{gas} = yield of producer gas (kg kg^{-1} of biomass in a dry and N_2-free basis)
y_{water} = yield of water (kg kg^{-1} of biomass in a dry basis)

Greek Symbols

β_0 = regression coefficient for the intercept term
β_1 = regression coefficient for the linear effect of pressure
β_2 = regression coefficient for the linear effect of peak temperature
β_{12} = regression coefficient for the interaction term
β_{11} = regression coefficient for the quadratic effect of pressure
β_{11} = regression coefficient for the quadratic effect of peak temperature
ρ = Pearson's correlation coefficient

Acronyms

BET = Brunauer−Emmett−Teller
CEC = cation exchange capacity
CP-MAS = cross polarization and magic angle spinning
DSC = differential scanning calorimetry
FC = fixed carbon
FCCCD = face centered central composite design
GC = gas chromatography
NMR = nuclear magnetic resonance
NTP = normal conditions
PID = proportional integral derivative
RSM = response surface methodology
TGA = thermogravimetric analysis
TPOMW = two-phase olive mill waste
XRF = X-ray fluorescence

REFERENCES

(1) Gaunt, J. L.; Lehmann, J. *Environ. Sci. Technol.* **2008**, *42*, 4152−4158.
(2) McHenry, M. P. *Agric., Ecosyst. Environ.* **2009**, *129*, 1−7.
(3) Manyà, J. J. *Environ. Sci. Technol.* **2012**, *46*, 7939−7954.
(4) Zhang, L.; Chunbao, X.; Champagne, P. *Energy Convers. Manage.* **2010**, *51*, 969−982.
(5) Brewer, C. E.; Schmidt-Rohr, K.; Satrio, J. A.; Brown, R. C. *Environ. Prog. Sustainable Energy* **2009**, *28*, 386−396.
(6) Antal, M. J.; Gronli, M. *Ind. Eng. Chem. Res.* **2003**, *42*, 1619−1640.
(7) Di Blasi, C.; Signorelli, G.; Di Russo, C.; Rea, G. *Ind. Eng. Chem. Res.* **1999**, *38*, 2216−2224.
(8) Demirbas, A. *J. Anal. Appl. Pyrolysis* **2004**, *72*, 243−248.
(9) Abdullah, H.; Wu, H. *Energy Fuels* **2009**, *23*, 4174−4181.

(10) Méndez, A.; Terradillos, M.; Gascó, G. *J. Anal. Appl. Pyrolysis* **2013**, *102*, 124−130.
(11) Duman, G.; Okutucu, C.; Ucar, S.; Stahl, R.; Yanik, J. *Bioresour. Technol.* **2011**, *102*, 1869−1878.
(12) Antal, M. J.; Allen, S. G.; Dai, X.; Shimizu, B.; Tam, M. S.; Gronli, M. *Ind. Eng. Chem. Res.* **2000**, *39*, 4024−4031.
(13) Enders, A.; Hanley, K.; Whitman, T.; Joseph, S.; Lehmann, J. *Bioresour. Technol.* **2012**, *114*, 644−653.
(14) Zhao, L.; Cao, X.; Mašek, O.; Zimmerman, A. *J. Hazard. Mater.* **2013**, *256*−*257*, 1−9.
(15) Manyà, J. J.; Roca, F. X.; Perales, J. F. *J. Anal. Appl. Pyrolysis* **2013**, *103*, 86−95.
(16) McBeath, A. V.; Smernik, R. J.; Schneider, M. P. W.; Schmidt, M. W. I.; Plant, E. L. *Org. Geochem.* **2011**, *42*, 1194−1202.
(17) Wu, W.; Yang, M.; Feng, Q.; McGrouther, K.; Wang, H.; Lu, H.; Chen, Y. *Biomass Bioenergy* **2012**, *47*, 268−276.
(18) Sun, H.; Hockaday, W. C.; Masiello, C. A.; Zygourakis, K. *Ind. Eng. Chem. Res.* **2012**, *51*, 3587−3597.
(19) Ghani, W. A. W. A. K.; Mohd, A.; da Silva, G.; Bachmann, R. T.; Taufiq-Yap, Y. H.; Rashid, U.; Al-Muhtaseb, A. H. *Ind. Crops Prod.* **2013**, *44*, 18−24.
(20) Pindoria, R. V.; Megaritis, A.; Messenböck, R. C.; Dugwell, D. R.; Kandiyoti, R. *Fuel* **1998**, *77*, 1247−1251.
(21) Antal, M. J.; Croiset, E.; Dai, X.; DeAlmeida, C.; Mok, W. S.; Niclas, N.; Richard, J. R.; Al Majthoub, M. *Energy Fuels* **1996**, *10*, 652−658.
(22) Mok, W. S.; Antal, M. J. *Thermochim. Acta* **1983**, *68*, 155−164.
(23) Rousset, P.; Figueiredo, C.; De Souza, M.; Quirino, W. *Fuel Process. Technol.* **2011**, *92*, 1890−1897.
(24) Melligan, F.; Auccaise, R.; Novotny, E. H.; Leahy, J. J.; Hayes, M. H. B.; Kwapinski, W. *Bioresour. Technol.* **2011**, *102*, 3466−3470.
(25) Aboyade, A. O.; Carrier, M.; Meyer, E. L.; Knoetze, H.; Görgens, J. F. *Energy Convers. Manage.* **2013**, *65*, 198−207.
(26) Fjellerup, J.; Gjernes, E.; Hansen, L. K. *Energy Fuels* **1996**, *10*, 649−651.
(27) Whitty, K.; Kullberg, M.; Sorvari, V.; Backman, R.; Hupa, M. *Bioresour. Technol.* **2008**, *99*, 671−679.
(28) Mahinpey, N.; Murugan, P.; Mani, T.; Raina, R. *Energy Fuels* **2009**, *23*, 2736−2742.
(29) Burhenne, L.; Messmer, J.; Aicher, T.; Laborie, M. *J. Anal. Appl. Pyrolysis* **2013**, *101*, 177−184.
(30) Roig, A.; Cayuela, M. L.; Sánchez-Monedero, M. A. *Waste Manage.* **2006**, *26*, 960−969.
(31) Cayuela, M. L.; Millner, P. D.; Meyer, S. L. F.; Roig, A. *Sci. Total Environ.* **2008**, *399*, 11−18.
(32) Yuan, J.; Xu, R.; Zhang, H. *Bioresour. Technol.* **2011**, *102*, 3488−3497.
(33) Singh, B. P.; Cowie, A. L.; Smernik, R. J. *Environ. Sci. Technol.* **2012**, *46*, 11770−11778.
(34) Montgomery, D. C. *Design and Analysis of Experiments*; Wiley: Hoboken, NJ, 2005.
(35) Grömping, U. *Tutorial for Designing Experiments Using the R Package RcmdrPlugin.DoE*; Report 4/2011; Reports in Mathematics, Physics and Chemistry; Beuth University of Applied Sciences: Berlin, 2011.
(36) Zimmerman, A. R. *Environ. Sci. Technol.* **2010**, *44*, 1295−1301.
(37) Mulligan, C. J.; Strezov, L.; Strezov, V. *Energy Fuels* **2010**, *24*, 46−52.
(38) Mašek, O.; Brownsort, P.; Cross, A.; Sohi, S. *Fuel* **2013**, *103*, 151−155.
(39) Wang, Y.; Hu, Y.; Zhao, X.; Wang, S.; Xing, G. *Energy Fuels* **2013**, *27*, 5890−5899.
(40) Lédé, J. *J. Anal. Appl. Pyrolysis* **2012**, *94*, 17−32.
(41) Yip, K.; Tian, F.; Hayashi, J. I.; Wu, H. *Energy Fuels* **2010**, *24*, 173−181.
(42) Dupont, C.; Nocquet, T.; Da Costa, J. A.; Verne-Tournon, C. *Bioresour. Technol.* **2011**, *102*, 9743−9748.
(43) Nanou, P.; Gutiérrez-Murillo, H. E.; van Swaaij, W. P. M.; van Rossum, G.; Kersten, S. R. A. *Chem. Eng. J.* **2013**, *217*, 289−299.
(44) Kaewpanha, M.; Guan, G.; Haoc, X.; Wang, Z.; Kasai, Y.; Kusakabe, K.; Abudula, A. *Fuel Process. Technol.* **2014**, *120*, 106−112.
(45) Manyà, J. J.; Laguarta, S.; Ortigosa, M. A. *Energy Fuels* **2013**, *27*, 5931−5939.
(46) Matsuoka, K.; Kajiwara, D.; Kuramoto, K.; Sharma, A.; Suzuki, Y. *Fuel Process. Technol.* **2009**, *90*, 895−900.
(47) Kim, K. H.; Kim, J.; Cho, T.; Choi, J. W. *Bioresour. Technol.* **2012**, *118*, 158−162.
(48) Keiluweit, M.; Nico, P. S.; Johnson, M. G.; Kleber, M. *Environ. Sci. Technol.* **2010**, *44*, 1247−1253.
(49) Crombie, K.; Masek, O.; Sohi, S. P.; Brownsort, P.; Cross, A. *GCB Bioenergy* **2013**, *5*, 122−131.
(50) Ronsse, F.; van Hecke, S.; Dickinson, D.; Prins, W. *GCB Bioenergy* **2013**, *5*, 104−115.
(51) Nguyen, B. T.; Lehmann, J.; Hockaday, W. C.; Joseph, S.; Masiello, C. A. *Environ. Sci. Technol.* **2010**, *44*, 3324−3331.
(52) Hammes, K.; Smernik, R. J.; Skjemstad, J. O.; Schmidt, M. W. I. *Appl. Geochem.* **2008**, *23*, 2113−2122.
(53) Rutherford, D. W.; Wershaw, R. L.; Rostad, C. E.; Kelly, C. N. *Biomass Bioenergy* **2012**, *46*, 693−701.
(54) Lee, Y.; Park, J.; Ryu, C.; Gang, K. S.; Yang, W.; Park, Y.; Jung, J.; Hyun, S. *Bioresour. Technol.* **2013**, *148*, 196−201.
(55) Hossain, M. K.; Strezov, V.; Chan, K. Y.; Ziolkowski, A.; Nelson, P. F. *J. Environ. Manage.* **2011**, *92*, 223−228.
(56) Mukherjee, A.; Zimmerman, A. R.; Harris, W. *Geoderma* **2011**, *163*, 247−255.
(57) Ragucci, R.; Giudicianni, P.; Cavaliere, A. *Fuel* **2013**, *107*, 122−130.
(58) Seshadri, K. S.; Shamsi, A. *Ind. Eng. Chem. Res.* **1998**, *37*, 3830−3837.
(59) Anis, S.; Zainal, Z. A. *Renewable Sustainable Energy Rev.* **2011**, *15*, 2355−2377.